SCIENCE CHINA
Information Sciences

• RESEARCH PAPER •

June 2026, Vol. 69, Iss. 6, 162101:1–162101:15
https://doi.org/10.1007/s11432-024-4569-1

Emergence of Metcalfe's law: mechanism and model

Cheng WANG[1,2,3*], Yi WANG[1,2] & Changjun JIANG[1,2,3*]

[1]*School of Computer Science and Technology, Tongji University, Shanghai 201804, China*
[2]*Key Laboratory of Embedded System and Service Computing, Ministry of Education, Shanghai 201804, China*
[3]*Shanghai Artificial Intelligence Laboratory, Shanghai 200232, China*

Received 29 August 2024/Revised 14 May 2025/Accepted 28 August 2025/Published online 27 April 2026

Abstract Metcalfe's law captures the relationship between the value of a network and its scale, asserting that the value of a network is directly proportional to the square of its size. Over the past four decades, researchers have proposed different scaling laws for network values. Remarkably, these seemingly conflicting conclusions have been substantiated by robust data validation, raising the question of which laws hold greater representativeness. Consequently, underlying mechanisms that underpin these laws are needed. This study aims to bridge this gap by offering a theoretical interpretation of Metcalfe's law and its variants. Based on a certain degree of consensus that *traffic is value*, network effects are gauged using network traffic load. A general analytical boundary for network traffic load is deduced by balancing practicality and analytical feasibility through the establishment of a comprehensive network model. From this foundation, the mechanism behind Metcalfe's law and its variants is elucidated, aligning the theoretical derivations with previously validated empirical evidence for Metcalfe's law.

Keywords network effect, Metcalfe's law, network behavior, network traffic load, scaling law

Citation Wang C, Wang Y, Jiang C J. Emergence of Metcalfe's law: mechanism and model. Sci China Inf Sci, 2026, 69(6): 162101, https://doi.org/10.1007/s11432-024-4569-1

1 Introduction

Among the various influential ideas that emerged during the Internet boom, Metcalfe's law [1] was one of the most significant. This law proposes that the value V of a network is directly proportional to the square of the number of its nodes n, that is, $V \propto n^2$, following a clear scaling law. Metcalfe's law is widely regarded as a universal empirical rule and has achieved prominent status. Similar to Moore's law, it is considered one of the five fundamental empirical laws that have stood the test of time [2]. In 1996, Reed Hundt, former chairman of the Federal Communications Commission, asserted that Metcalfe's and Moore's laws provided the foundation for the comprehension of the Internet [3]. With the emergence of Metcalfe's law, further research has been conducted. Studies on Metcalfe's law in the context of network effects have become a contentious subject in various explorations [4–10]. Several other laws have also been proposed [4–6, 8, 10, 11]. These laws can be classified into Reed's [4], Sarnoff's [5], and Odlyzko's [6] laws. These formulations are denoted as $V \propto 2^n$, $V \propto n$, and $V \propto n \log n$, respectively. As all these laws describe the relationship between network value and scale, we refer to them as variants of Metcalfe's law.

Metcalfe's law is a fundamental empirical principle for understanding technological growth. It has been applied across a wide range of domains, from traditional communication systems to modern web applications and social networks [12]. This significantly influences digital blockchain networks and cryptocurrency valuations, including Bitcoin analysis [13–15]. Jung et al. [16] demonstrated that social network services tend to follow a polynomial adoption curve based on web traffic. Scala et al. [17] highlighted the explosive growth in network value. Ma et al. [18] examined the nonlinear impact of Metcalfe's law on the digitization of a green economy. Tang et al. [19] introduced the DERVA (discounted equity valuation analysis) method for enterprise valuation using Metcalfe's law. Assif et al. [20] analyzed crowdsourcing network value distribution fairness. Moro-Visconti [21] applied this law to the COVID-19 healthcare digital transformation. Nowak [22] integrated network laws into urban platform coordination systems.

A series of data validation studies [4,5,10,12–15] have confirmed Metcalfe's law and its variants separately, creating a debate over the scaling law that holds greater representativeness. In addition, Zhang et al. [23] reevaluated the

* Corresponding author (email: cwang@tongji.edu.cn, cjjiang@tongji.edu.cn)

most recent data from Facebook and Tencent in 2023, revealing that the cube law ($V \propto n^3$) offered a more precise representation of actual network values than Metcalfe's law.

Despite empirical confirmation, the reason these laws consistently hold true in data validation remains an unresolved question. Moreover, which laws that most accurately describe the relationship between the value of a network and the number of its nodes remain unclear. These questions cannot be solved through empirical research, and therefore, addressing them is crucial for advancing the understanding of networks. A thorough understanding of the relationship between network value and size, as well as a demonstration of the general applicability of this research, requires the establishment of a series of mechanisms capable of reproducing these laws.

In this study, we use the measurement of network traffic as a fundamental metric for assessing the value of networks within the scope of mechanism modeling [16, 24], aligning with the principle that *traffic is value*. This principle is evident in practical applications, such as Internet service providers (ISPs) and cloud computing. In many countries, ISPs have transitioned from a flat-fee model to usage-based billing to fund the deployment of more bandwidth, particularly from video streaming, owing to increasing Internet traffic [25]. Similarly, in cloud computing, the rapid expansion of services has led to increasing operational costs, with bandwidth costs being a significant factor [26–31]. Expanding on this insight, we rely on the network traffic load as a crucial indicator for evaluating the worth of networks. The reasoning behind this choice is in the fact that a higher traffic load signifies an increased network capacity to accommodate nodes, consequently enhancing the overall value of the network.

2 Problem formulation

Here, we report the generation of the network and its underlying mechanisms. We consider a general network model in which all nodes can be considered as both sources and users of data, capable of generating and receiving data. We outline this network structure and define the traffic load accordingly. A network architecture is proposed comprising two layers, that is, the underlying and overlying layers, as shown in Figure 1. The underlying layer is dedicated to the physical transmission of data, whereas the overlying layer facilitates the interactions between devices and users. This study emphasizes the examination of the information transmission load, specifically within the overlying layer, and explores the intricacies and effects of this load on the network performance and overall system behavior. By analyzing the information transmission load in the overlying layer, we can gain deeper insights into the transmission patterns of the network architecture.

The true value of a network is in fulfilling the requirements of its nodes. Unlike an isolated node that operates independently, the purpose of a network is to satisfy the needs of nodes through data transmission. Data transmission results in traffic, which, in turn, emerges as a key indicator of the value of a network. Thus, the value of the network becomes evident through the volume of network traffic. Rajgopal et al. [24] found that the relationship between traffic and network economy, which is related to Metcalfe's law, uses *traffic load* as a metric of network value.

We consider a network comprising a random number N (with $\mathbb{E}[N] = n$) of nodes distributed within a square region. Wraparound conditions are applied at the edges of the region by treating the network as the surface of a two-dimensional torus $\mathcal{O}$ to avoid border effects. We assume that the number of nodes is exactly n to simplify the problem; without affecting the result in order sense, we denote the set of nodes u_k $(k = 1, 2, \ldots, n)$ as $\mathcal{U}$.

For each node u_k, the traffic load for a data transportation session T_k (e.g., broadcast) over N is defined as follows: $\mathrm{L}_{\mathrm{N}}^{\mathrm{T}_k} = \lambda_k \cdot d_{\mathrm{S_N},u_k}$, where λ_k is the data arrival rate of node u_k, and $d_{\mathrm{S_N},u_k}$ indicates the aggregated distance data transporting from u_k to destinations of T_k over network N under a given data transportation scheme $\mathrm{S_N}$.

3 Generation mechanisms of traffic load

Four key aspects to network traffic load exist. We first define the overall structure and geographical distribution of the network to ensure completeness. We then consider the various components of the network. From a relational perspective, we account for the degree of closeness and define the separation of relationships. Next, we analyze the influence of different types of nodes, beginning with the nodes themselves. Based on the data transmission choices of the generators and interests of the receivers, we define the distribution of data destinations within the network.

These four distributions carry distinct meanings and serve complementary roles; however, they are intrinsically interconnected in shaping the behavior of network information transmission. Network geographic distribution describes the correlation between node relationship formation and the spatial arrangement of nodes. This provides a foundation for understanding the influence of geographical and infrastructural factors on connectivity. Building on this, the relationship separation distribution captures the link between distance and topological characteristics. This

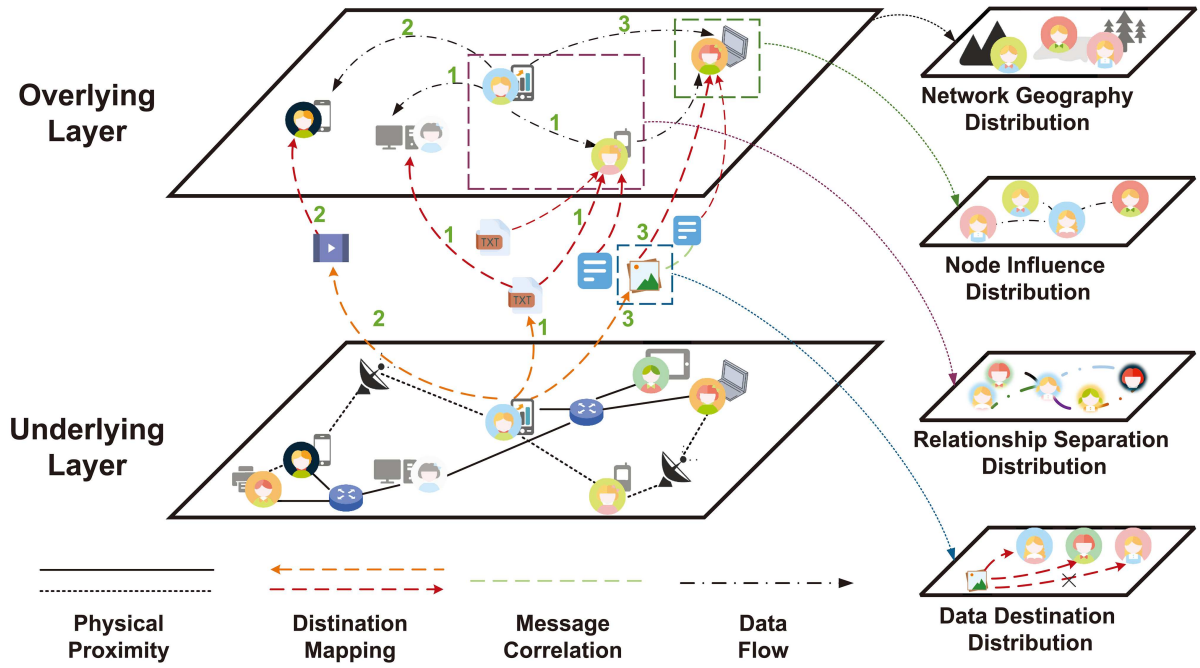

Figure 1 (Color online) Proposed two-layer network model. The underlying layer handles physical data transmission, whereas the overlying layer facilitates device/user interactions. This work introduces four parameters to provide an understanding for the completeness of the overlying layer.

reflects how the structural layout influences the dynamic interactions. We introduce anchor points into a continuous space from which the actual neighbors are determined based on proximity to achieve a more realistic selection of neighboring nodes. The node influence distribution models the behavior of source nodes during communication sessions. In this context, a source disseminates information to all directly connected nodes (e.g., followers or friends), effectively quantifying its broadcasting reach. Finally, the data destination distribution refines the broadcasting process by selecting the nodes that receive information. This selection is based on the latent social relevance or contextual association between the source and destination nodes.

3.1 Network geography distribution

Considering networks covering regions with relatively uniform distribution densities, we assume the model to be a *homogeneous random extended network*, as in [32, 33]. The definition of the network geography distribution can be extended to general network models, such as the clustering random model [34] constructed using the following procedure. First, the center of $\mathcal{O}$ is the center point, denoted by O. Subsequently, the center point O generates a point process for nodes whose local intensity at position X is given by $\mathbf{d}(X) = n \cdot \kappa(O, X)$, where $\kappa(O, X)$ is the dispersion density function. Moreover, we assume that $\kappa(O, \cdot)$ is a summable, nonincreasing, bounded, and continuous function, and $\int_{\mathcal{O}} \kappa(O, X)dX = 1$. Following a common normalization method, $\kappa(O, \cdot)$ can be specified by first defining a nonincreasing, bounded, and continuous function $g(s)$ as $\kappa(O, X) = \frac{g(|X-O|)}{\int_{\mathcal{O}} g(|Y-O|)dY}$. Specifically, the clustering function is defined as $g(s) := \min\{1, s^{-\mathfrak{g}}\}$, where $\mathfrak{g}$ is an exponent binding the function. This satisfies the assumption that $\mathfrak{g} = 0$ and $g(s) = 1$ correspond to uniform distributions.

3.2 Relationship separation distribution

For the relationship separation distribution, let $\mathcal{D}(u, r)$ represent the disk with the center at a point u and radius r within the deployment region $\mathcal{O}$, and define $N(u, r)$ as the number of nodes within $\mathcal{D}(u, r)$. Kleinberg [35] proposed a distance-based social model related to geographical distance and social friendships, whereas Liben-Nowell et al. [36] introduced a rank-based model. The rank-based model states that friendship probability depends on geographic distance and node density. We use a population-based model [34] by modifying the rank-based model. It is convenient to bind the total length of the Euclidean spanning trees using the following derivation. Considering node v_k as the reference point, this distribution can independently select q_k points within the torus region $\mathcal{O}$ using

a density function [34]

$$f_{v_k}(X) = \Phi_k(S, \mathfrak{s}) \cdot (\mathbb{E}[N(v_k, |X - v_k|)] + 1)^{-\mathfrak{s}}, \tag{1}$$

where the position of a selected point in region $\mathcal{O}$ is denoted by the random variable X, and $|X - v_k|$ represents the Euclidean distance between X and v_k. The relationship separation exponent is represented by $\mathfrak{s} \in [0, \infty)$, and the coefficient $\Phi_k(S, \mathfrak{s}) > 0$ depends on both the area S of regions $\mathcal{O}$ and $\mathfrak{s}$, satisfying $\Phi_k(S, \mathfrak{s}) \cdot \int_{\mathcal{O}} (\mathbb{E}[N(v_k, |X - v_k|)] + 1)^{-\mathfrak{s}} dX = 1$.

From the population-based model, node v_k and q_k neighbor nodes are selected using the following procedure. First, we independently select q_k anchor points for node v_k according to the relationship separation distribution, denoted as $\mathcal{A}_k = \{p_{k_1}, p_{k_2}, \ldots, p_{k_{q_k}}\}$. These points are sampled within a continuous plane to ensure the analytical tractability of the model. Then, based on the nearest-neighbor principle, we identify the q_k neighbor nodes of node v_k that correspond to these anchor points. This approach maintains the feasibility of the analysis and its consistency with real-world scenarios.

Incorporating an exponent enhances the insight into the node distribution across distances from a central node, considering the number of hops to reflect the relationship proximity. This approach is crucial in social networks, where physical distance does not restrict connections. This is also important in telecom networks, where the operational range is limited. We can assess the extent of the service and understand the spatial coverage and concentration of network resources by quantifying the clustering exponent.

3.3 Node influence distribution

Real-life scenarios often exhibit a pattern in which only a limited number of nodes have high degrees of connectivity, whereas the majority of nodes have relatively lower degrees. For instance, in online social networks, most people are primarily connected to those they know well, whereas a small subset of users, such as celebrities, may have numerous connections. Under this assumption, the number of neighboring nodes q_k for a given node v_k follows a Zipf's distribution [37, 38], that is, $\Pr(q_k = q) \propto q^{-\mathfrak{i}}$, where $\mathfrak{i}$ serves as an exponent in node influence distribution. Independent of the network system and the identity of its constituents, the probability $\Pr(q_k = q)$ that a vertex in the network interacts with q of the other vertices decays as a power law. A power-law distribution is a reasonable approach for capturing this characteristic, because it corresponds to the observed pattern of a few nodes exhibiting high degrees, whereas the majority of nodes exhibit lower connectivity levels.

3.4 Data destination distribution

The distribution of destinations in the network exhibits characteristics similar to Zipf's distribution [37,38], denoted as r_k. Mathematically, $\Pr(r_k = r \mid q_k = q) \propto r^{-\mathfrak{d}}$, where r_k represents the number of destinations for a data transmission session from node v_k and $\mathfrak{d}$ denotes the exponent of the data destination distribution. This conditional probability formulation arises because the number of destinations r_k is influenced by session-specific characteristics, represented by q_k. From the perspective of data generators, a typical example is a delivery network, where the destination for data delivery is predetermined at the moment of data generation, and the data generators are responsible for determining who receives the data. A typical example of this scenario, from the perspective of data receivers, is an online social network [34]. Users genuinely interested in specific content resolve to accept and interact with the content shared by the central users. This introduces a certain degree of randomness to the number of data destinations. The data destination distribution was used to synthesize the above situations.

Employing a model that integrates these four components demonstrates that they are the causes of the power-law scaling of the traffic load observed in actual networks. These components play a readily recognizable and significant role in the development of numerous networks, suggesting that these findings are pertinent to a large class of networks.

4 Derivation of traffic load

Next, we show that a model based on the four distributions mentioned in Section 3 naturally leads to the scaling behavior of the network traffic load, thereby connecting it to Metcalfe's law and its variants.

The following theorem demonstrates a theoretical bound on the traffic load for a network N.

Theorem 1. Let $\mathrm{L}_{\mathrm{N}}^*$ denote the traffic load for data transportation in a network N with n nodes. It holds that

$$\mathrm{L}_{\mathrm{N}}^* = \mathrm{L}_{\mathrm{N}}^*(\lambda, \mathfrak{i}, \mathfrak{s}, \mathfrak{d}, n),$$

Table 1 Results on the traffic load $\mathrm{L}_{\mathrm{N}}^{*}$ and labeling of scaling laws under $\lambda=\Theta(1)$. Different theoretical results derived from the distributions above. We use double underscores to indicate Metcalfe's law, single underscores for Sarnoff's law, and tildes for Odlyzko's law, respectively.

$\mathfrak{d}\setminus\mathfrak{s}$	$\mathfrak{s}>2$	$\mathfrak{s}=2$	$1<\mathfrak{s}<2$	$\mathfrak{s}=1$	$0\leqslant\mathfrak{s}<1$
$\mathfrak{d}>2$	$\underline{\lambda\cdot\Omega(n)}$, $\mathfrak{i}\geqslant 0$	$\underline{\underline{\lambda\cdot\Omega(n\log n)}}$, $\mathfrak{i}\geqslant 0$	$\lambda\cdot\Omega(n^{2-\frac{\mathfrak{s}}{2}})$, $\mathfrak{i}\geqslant 0$	$\lambda\cdot\Omega(n^{\frac{3}{2}}/\sqrt{\log n})$, $\mathfrak{i}\geqslant 0$	$\lambda\cdot\Omega(n^{\frac{3}{2}})$, $\mathfrak{i}\geqslant 0$
$\mathfrak{d}=2$	$\begin{cases}\underline{\lambda\cdot\Omega(n)},\\ \quad \mathfrak{i}>1;\\ \underline{\underline{\lambda\cdot\Omega(n\log n)}},\\ \quad 0\leqslant\mathfrak{i}\leqslant 1\end{cases}$	$\underline{\underline{\lambda\cdot\Omega(n\log n)}}$, $\mathfrak{i}\geqslant 0$	$\lambda\cdot\Omega(n^{2-\frac{\mathfrak{s}}{2}})$, $\mathfrak{i}\geqslant 0$	$\lambda\cdot\Omega(n^{\frac{3}{2}}/\sqrt{\log n})$, $\mathfrak{i}\geqslant 0$	$\lambda\cdot\Omega(n^{\frac{3}{2}})$, $\mathfrak{i}\geqslant 0$
$\frac{3}{2}<\mathfrak{d}<2$	$\begin{cases}\underline{\lambda\cdot\Omega(n)},\\ \quad \mathfrak{i}>3-\mathfrak{d};\\ \underline{\underline{\lambda\cdot\Omega(n\log n)}},\\ \quad \mathfrak{i}=3-\mathfrak{d};\\ \lambda\cdot\Omega(n^{4-\mathfrak{i}-\mathfrak{d}}),\\ \quad 1<\mathfrak{i}<3-\mathfrak{d};\\ \lambda\cdot\Omega(n^{3-\mathfrak{d}}/\log n),\\ \quad \mathfrak{i}=1;\\ \lambda\cdot\Omega(n^{3-\mathfrak{d}}),\\ \quad 0\leqslant\mathfrak{i}<1\end{cases}$	$\begin{cases}\underline{\underline{\lambda\cdot\Omega(n\log n)}},\\ \quad \mathfrak{i}\geqslant 3-\mathfrak{d};\\ \lambda\cdot\Omega(n^{4-\mathfrak{i}-\mathfrak{d}}),\\ \quad 1<\mathfrak{i}<3-\mathfrak{d};\\ \lambda\cdot\Omega(n^{3-\mathfrak{d}}/\log n),\\ \quad \mathfrak{i}=1;\\ \lambda\cdot\Omega(n^{3-\mathfrak{d}}),\\ \quad 0\leqslant\mathfrak{i}<1\end{cases}$	$\begin{cases}\lambda\cdot\Omega(n^{2-\frac{\mathfrak{s}}{2}}),\\ \quad \mathfrak{i}\geqslant 3-\mathfrak{d};\\ \lambda\cdot\Omega(n^{4-\mathfrak{i}-\mathfrak{d}}),\\ \quad 1<\mathfrak{i}<3-\mathfrak{d};\\ \lambda\cdot\Omega(n^{3-\mathfrak{d}}/\log n),\\ \quad \mathfrak{i}=1;\\ \lambda\cdot\Omega(n^{3-\mathfrak{d}}),\\ \quad 0\leqslant\mathfrak{i}<1\end{cases}$	$\lambda\cdot\Omega(n^{\frac{3}{2}}/\sqrt{\log n})$, $\mathfrak{i}\geqslant 0$	$\lambda\cdot\Omega(n^{\frac{3}{2}})$, $\mathfrak{i}\geqslant 0$
$\mathfrak{d}=\frac{3}{2}$	$\begin{cases}\underline{\lambda\cdot\Omega(n)},\\ \quad \mathfrak{i}>\frac{3}{2};\\ \underline{\underline{\lambda\cdot\Omega(n\log n)}},\\ \quad \mathfrak{i}=\frac{3}{2};\\ \lambda\cdot\Omega(n^{\frac{5}{2}-\mathfrak{i}}),\\ \quad 1<\mathfrak{i}<\frac{3}{2};\\ \lambda\cdot\Omega(n^{\frac{3}{2}}/\log n),\\ \quad \mathfrak{i}=1;\\ \lambda\cdot\Omega(n^{\frac{3}{2}}),\\ \quad 0\leqslant\mathfrak{i}<1\end{cases}$	$\begin{cases}\underline{\underline{\lambda\cdot\Omega(n\log n)}},\\ \quad \mathfrak{i}\geqslant\frac{3}{2};\\ \lambda\cdot\Omega(n^{\frac{5}{2}-\mathfrak{i}}),\\ \quad 1<\mathfrak{i}<\frac{3}{2};\\ \lambda\cdot\Omega(n^{\frac{3}{2}}/\log n),\\ \quad \mathfrak{i}=1;\\ \lambda\cdot\Omega(n^{\frac{3}{2}}),\\ \quad 0\leqslant\mathfrak{i}<1\end{cases}$	$\begin{cases}\lambda\cdot\Omega(n^{2-\frac{\mathfrak{s}}{2}}),\\ \quad \mathfrak{i}\geqslant\frac{3}{2};\\ \lambda\cdot\Omega(n^{\frac{5}{2}-\mathfrak{i}}),\\ \quad 1<\mathfrak{i}<\frac{3}{2};\\ \lambda\cdot\Omega(n^{\frac{3}{2}}/\log n),\\ \quad \mathfrak{i}=1;\\ \lambda\cdot\Omega(n^{\frac{3}{2}}),\\ \quad 0\leqslant\mathfrak{i}<1\end{cases}$	$\begin{cases}\lambda\cdot\Omega(n^{\frac{3}{2}}/\sqrt{\log n}),\\ \quad \mathfrak{i}>1;\\ \lambda\cdot\Omega(n^{\frac{3}{2}}\sqrt{\log n}),\\ \quad 0\leqslant\mathfrak{i}\leqslant 1\end{cases}$	$\begin{cases}\lambda\cdot\Omega(n^{\frac{3}{2}}),\\ \quad \mathfrak{i}>1;\\ \lambda\cdot\Omega(n^{\frac{3}{2}}\log n),\\ \quad 0\leqslant\mathfrak{i}\leqslant 1\end{cases}$
$1<\mathfrak{d}<\frac{3}{2}$	$\begin{cases}\underline{\lambda\cdot\Omega(n)},\\ \quad \mathfrak{i}>3-\mathfrak{d};\\ \underline{\underline{\lambda\cdot\Omega(n\log n)}},\\ \quad \mathfrak{i}=3-\mathfrak{d};\\ \lambda\cdot\Omega(n^{4-\mathfrak{i}-\mathfrak{d}}),\\ \quad 1<\mathfrak{i}<3-\mathfrak{d};\\ \lambda\cdot\Omega(n^{3-\mathfrak{d}}/\log n),\\ \quad \mathfrak{i}=1;\\ \lambda\cdot\Omega(n^{3-\mathfrak{d}}),\\ \quad 0\leqslant\mathfrak{i}<1\end{cases}$	$\begin{cases}\underline{\underline{\lambda\cdot\Omega(n\log n)}},\\ \quad \mathfrak{i}\geqslant 3-\mathfrak{d};\\ \lambda\cdot\Omega(n^{4-\mathfrak{i}-\mathfrak{d}}),\\ \quad 1<\mathfrak{i}<3-\mathfrak{d};\\ \lambda\cdot\Omega(n^{3-\mathfrak{d}}/\log n),\\ \quad \mathfrak{i}=1;\\ \lambda\cdot\Omega(n^{3-\mathfrak{d}}),\\ \quad 0\leqslant\mathfrak{i}<1\end{cases}$	$\begin{cases}\lambda\cdot\Omega(n^{2-\frac{\mathfrak{s}}{2}}),\\ \quad \mathfrak{i}\geqslant 3-\mathfrak{d};\\ \lambda\cdot\Omega(n^{4-\mathfrak{i}-\mathfrak{d}}),\\ \quad 1<\mathfrak{i}<3-\mathfrak{d};\\ \lambda\cdot\Omega(n^{3-\mathfrak{d}}/\log n),\\ \quad \mathfrak{i}=1;\\ \lambda\cdot\Omega(n^{3-\mathfrak{d}}),\\ \quad 0\leqslant\mathfrak{i}<1\end{cases}$	$\begin{cases}\lambda\cdot\Omega(n^{\frac{3}{2}}/\sqrt{\log n}),\\ \quad \mathfrak{i}>\frac{5}{2}-\mathfrak{d};\\ \lambda\cdot\Omega(n^{\frac{3}{2}}\sqrt{\log n}),\\ \quad \mathfrak{i}=\frac{5}{2}-\mathfrak{d};\\ \lambda\cdot\Omega(n^{4-\mathfrak{i}-\mathfrak{d}}),\\ \quad 1<\mathfrak{i}<\frac{5}{2}-\mathfrak{d};\\ \lambda\cdot\Omega(n^{3-\mathfrak{d}}/\log n),\\ \quad \mathfrak{i}=1;\\ \lambda\cdot\Omega(n^{3-\mathfrak{d}}),\\ \quad 0\leqslant\mathfrak{i}<1\end{cases}$	$\begin{cases}\lambda\cdot\Omega(n^{\frac{3}{2}}),\\ \quad \mathfrak{i}>\frac{5}{2}-\mathfrak{d};\\ \lambda\cdot\Omega(n^{\frac{3}{2}}\cdot\log n),\\ \quad \mathfrak{i}=\frac{5}{2}-\mathfrak{d};\\ \lambda\cdot\Omega(n^{4-\mathfrak{i}-\mathfrak{d}}),\\ \quad 1<\mathfrak{i}<\frac{5}{2}-\mathfrak{d};\\ \lambda\cdot\Omega(n^{3-\mathfrak{d}}/\log n),\\ \quad \mathfrak{i}=1;\\ \lambda\cdot\Omega(n^{3-\mathfrak{d}}),\\ \quad 0\leqslant\mathfrak{i}<1\end{cases}$
$\mathfrak{d}=1$	$\begin{cases}\underline{\lambda\cdot\Omega(n)},\\ \quad \mathfrak{i}\geqslant 2;\\ \lambda\cdot\Omega(n^{3-\mathfrak{i}}/\log n),\\ \quad 1<\mathfrak{i}<2;\\ \lambda\cdot\Omega(n^2/(\log n)^2),\\ \lambda\cdot\Omega(n^2/\log n),\\ \quad 0\leqslant\mathfrak{i}<1\end{cases}$	$\begin{cases}\underline{\underline{\lambda\cdot\Omega(n\log n)}},\\ \quad \mathfrak{i}\geqslant 2;\\ \lambda\cdot\Omega(n^{3-\mathfrak{i}}/\log n),\\ \quad 1<\mathfrak{i}<2;\\ \lambda\cdot\Omega(n^2/(\log n)^2),\\ \quad \mathfrak{i}=1;\\ \lambda\cdot\Omega(n^2/\log n),\\ \quad 0\leqslant\mathfrak{i}<1\end{cases}$	$\begin{cases}\lambda\cdot\Omega(n^{2-\frac{\mathfrak{s}}{2}}),\\ \quad \mathfrak{i}\geqslant 2;\\ \lambda\cdot\Omega(n^{3-\mathfrak{i}}/\log n),\\ \quad 1<\mathfrak{i}<2;\\ \lambda\cdot\Omega(n^2/(\log n)^2),\\ \quad \mathfrak{i}=1;\\ \lambda\cdot\Omega(n^2/\log n),\\ \quad 0\leqslant\mathfrak{i}<1\end{cases}$	$\begin{cases}\lambda\cdot\Omega(n^{\frac{3}{2}}/\sqrt{\log n}),\\ \quad \mathfrak{i}\geqslant 2;\\ \lambda\cdot\Omega(n^{3-\mathfrak{i}}/\log n),\\ \quad 1<\mathfrak{i}<2;\\ \lambda\cdot\Omega(n^2/(\log n)^2),\\ \quad \mathfrak{i}=1;\\ \lambda\cdot\Omega(n^2/\log n),\\ \quad 0\leqslant\mathfrak{i}<1\end{cases}$	$\begin{cases}\lambda\cdot\Omega(n^{\frac{3}{2}}),\\ \quad \mathfrak{i}\geqslant 2;\\ \lambda\cdot\Omega(n^{3-\mathfrak{i}}/\log n),\\ \quad 1<\mathfrak{i}<2;\\ \lambda\cdot\Omega(n^2/(\log n)^2),\\ \quad \mathfrak{i}=1;\\ \lambda\cdot\Omega(n^2/\log n),\\ \quad 0\leqslant\mathfrak{i}<1\end{cases}$
$0\leqslant\mathfrak{d}<1$	$\begin{cases}\underline{\lambda\cdot\Omega(n)},\\ \underline{\underline{\lambda\cdot\Omega(n\log n)}},\\ \quad \mathfrak{i}=2;\\ \lambda\cdot\Omega(n^{3-\mathfrak{i}}),\\ \quad 1<\mathfrak{i}<2;\\ \lambda\cdot\Omega(n^2/\log n),\\ \quad \mathfrak{i}=1;\\ \underline{\underline{\lambda\cdot\Omega(n^2)}},\\ \quad 0\leqslant\mathfrak{i}<1\end{cases}$	$\begin{cases}\underline{\underline{\lambda\cdot\Omega(n\log n)}},\\ \quad \mathfrak{i}\geqslant 2;\\ \lambda\cdot\Omega(n^{3-\mathfrak{i}}),\\ \quad 1<\mathfrak{i}<2;\\ \lambda\cdot\Omega(n^2/\log n),\\ \quad \mathfrak{i}=1;\\ \underline{\underline{\lambda\cdot\Omega(n^2)}},\\ \quad 0\leqslant\mathfrak{i}<1\end{cases}$	$\begin{cases}\lambda\cdot\Omega(n^{2-\frac{\mathfrak{s}}{2}}),\\ \quad \mathfrak{i}\geqslant 2;\\ \lambda\cdot\Omega(n^{3-\mathfrak{i}}),\\ \quad 1<\mathfrak{i}<2;\\ \lambda\cdot\Omega(n^2/\log n),\\ \quad \mathfrak{i}=1;\\ \underline{\underline{\lambda\cdot\Omega(n^2)}},\\ \quad 0\leqslant\mathfrak{i}<1\end{cases}$	$\begin{cases}\lambda\cdot\Omega(n^{\frac{3}{2}}/\sqrt{\log n}),\\ \quad \mathfrak{i}>\frac{3}{2};\\ \lambda\cdot\Omega(n^{\frac{3}{2}}\sqrt{\log n}),\\ \quad \mathfrak{i}=\frac{3}{2};\\ \lambda\cdot\Omega(n^{3-\mathfrak{i}}),\\ \quad 1<\mathfrak{i}<\frac{3}{2};\\ \lambda\cdot\Omega(n^2/\log n),\\ \quad \mathfrak{i}=1;\\ \underline{\underline{\lambda\cdot\Omega(n^2)}},\\ \quad 0\leqslant\mathfrak{i}<1\end{cases}$	$\begin{cases}\lambda\cdot\Omega(n^{\frac{3}{2}}),\\ \quad \mathfrak{i}>\frac{3}{2};\\ \lambda\cdot\Omega(n^{\frac{3}{2}}\cdot\log n),\\ \quad \mathfrak{i}=\frac{3}{2};\\ \lambda\cdot\Omega(n^{3-\mathfrak{i}}),\\ \quad 1<\mathfrak{i}<\frac{3}{2};\\ \lambda\cdot\Omega(n^2/\log n),\\ \quad \mathfrak{i}=1;\\ \underline{\underline{\lambda\cdot\Omega(n^2)}},\\ \quad 0\leqslant\mathfrak{i}<1\end{cases}$

where the value of $\mathrm{L}_{\mathrm{N}}^{*}$, presented in Table 1, depends on the data arrival/generation rate λ, the exponent of node-influence distribution $\mathfrak{i}$, the exponent of relationship separation distribution $\mathfrak{s}$, and the exponent of data destination distribution $\mathfrak{d}$.

Table 2 Some exemplary possible cases of the representative scaling laws under the assumption that a linear relationship exists between the value and traffic load of networks.

Representative scaling laws	Some exemplary possible cases
Metcalfe's law: n^2	$\lambda=\Theta(1), \mathfrak{s}\geqslant 0, 0\leqslant \mathfrak{d}<1, 0\leqslant \mathfrak{i}<1;$ $\lambda=\Theta(n^{1/2}), 0\leqslant \mathfrak{s}<1, \mathfrak{d}>3/2, \mathfrak{i}\geqslant 0;$ $\lambda=\Theta(n^{1/2}), 0\leqslant \mathfrak{s}<1, \mathfrak{d}=3/2, \mathfrak{i}>1;$ $\lambda=\Theta(n^{1/2}), 0\leqslant \mathfrak{s}<1, 1<\mathfrak{d}<3/2, \mathfrak{i}>5/2-\mathfrak{d};$ $\lambda=\Theta(n^{1/2}), 0\leqslant \mathfrak{s}<1, \mathfrak{d}=1, \mathfrak{i}\geqslant 2;$ $\lambda=\Theta(n^{1/2}), 0\leqslant \mathfrak{s}<1, 0\leqslant \mathfrak{d}<1, \mathfrak{i}>3/2$
Sarnoff's law: n	$\lambda=\Theta(1), \mathfrak{s}>2, \mathfrak{d}>2, \mathfrak{i}\geqslant 0;$ $\lambda=\Theta(1), \mathfrak{s}>2, \mathfrak{d}=2, \mathfrak{i}>1;$ $\lambda=\Theta(1), \mathfrak{s}>2, 1<\mathfrak{d}<2, \mathfrak{i}>3-\mathfrak{d};$ $\lambda=\Theta(1), \mathfrak{s}>2, \mathfrak{d}=1, \mathfrak{i}\geqslant 2;$ $\lambda=\Theta(1), \mathfrak{s}>2, 0\leqslant \mathfrak{d}<1, \mathfrak{i}>2$
Odlyzko's law: $n\log n$	$\lambda=\Theta(1), \mathfrak{s}=2, \mathfrak{d}\geqslant 2, \mathfrak{i}\geqslant 0;$ $\lambda=\Theta(1), \mathfrak{s}>2, \mathfrak{d}=2, 0\leqslant \mathfrak{i}<1;$ $\lambda=\Theta(1), \mathfrak{s}=2, 1\leqslant \mathfrak{d}<2, \mathfrak{i}\geqslant 3-\mathfrak{d};$ $\lambda=\Theta(1), \mathfrak{s}>2, 0\leqslant \mathfrak{d}<1, \mathfrak{i}=2;$ $\lambda=\Theta(1), \mathfrak{s}=2, 0\leqslant \mathfrak{d}<1, \mathfrak{i}\geqslant 2$
Cube law: n^3	$\lambda=\Theta(n), \mathfrak{s}\geqslant 0, 0\leqslant \mathfrak{d}<1, 0\leqslant \mathfrak{i}<1$

We provide a sketch of the proof. Starting with p_k nodes, a set of anchor points $\mathcal{A}_k$ was constructed from the relationship separation distribution by applying the node influence distribution. Because not all neighboring nodes can obtain this information, the number of transmission destinations follows a data destination distribution. Based on $\mathcal{P}_k := \{v_k\}\cup\mathcal{A}_k$, the Euclidean minimum spanning tree (EMST) can be constructed using classic greedy algorithms such as Prim. It provides a framework that minimizes the total distance between all the points in the network while maintaining a connected structure.

A comprehensive and nuanced understanding of traffic load can be obtained by integrating these methodologies, including determining destinations, selecting anchor points, and constructing an EMST. The traffic load satisfies the following: $\mathrm{L}_{\mathrm{N}}^{*}=\lambda\cdot\Omega\left(\sum_{k=1}^{n}|\,\mathrm{EMST}(\{u_k\}\cup\mathbb{D}_k)|\right)$, where λ denotes the data arrival rate, $\mathrm{EMST}(\cdot)$ denotes the EMST over a set, and $\mathbb{D}_k$ represents all the destinations of u_k. To compute this, we consider whether q_k has a constant influence $\Theta(1)$. When $q_k=\Theta(1)$, the EMST is held at the aggregated distance between u_k and the set of anchor points. When $q_k=\omega(1)$, we further consider r_k. For $r_k=\Theta(1)$, the order of the results is lower than that for $q_k=\Theta(1)$. For $r_k=\omega(1)$, the number of destinations is not constant, and we sum all destinations.

Finally, we integrate both the network geographical distribution and relationship separation distribution into the proposed model. Specifically, we assume uniform network geography by setting $\mathfrak{g}=0$. For the relationship separation distribution, we further examine the density function that governs the selection of the nearest neighbor set for each source node. The total length of the EMST is computed from the relationship separation distribution.

5 Reproducing Metcalfe's law

These distributions are common to a number of complex networks, including social and transportation networks. Consequently, it is reasonable to interpret Metcalfe's law and its variants as emergent results of the combined effects of these mechanisms.

Possible cases associated with Metcalfe's law are summarized in Table 2. This illustrates scenarios in which Metcalfe's law holds for different values of λ. Notably, when $\lambda=\Theta(1)$, we observe a consistent alignment with Metcalfe's law for $\mathfrak{s}\geqslant 0$, $0\leqslant\mathfrak{d}<1$, and $0\leqslant\mathfrak{i}<1$. This suggests that provided the network has a positive exponent parameter $\mathfrak{s}$ and a significant number of active users, Metcalfe's law is applicable for describing its growth and value creation. A typical example is online social networks, such as Facebook and Tencent, which have extensive user bases and high user engagement.

Furthermore, we explore the case of $\lambda=\Theta(n^{1/2})$ and indicate five distinct scenarios that yield similar conclusions. With the advancement of the Internet, it has become increasingly clear that the scale of networks is continuously expanding. Simultaneously, the speed of data transmission within these networks has increased. This growth is reflected in two key aspects. First, the number of connected users and devices has increased. Second, the growth is also evident in the development of the supporting infrastructure, including routers, switches, and servers, which

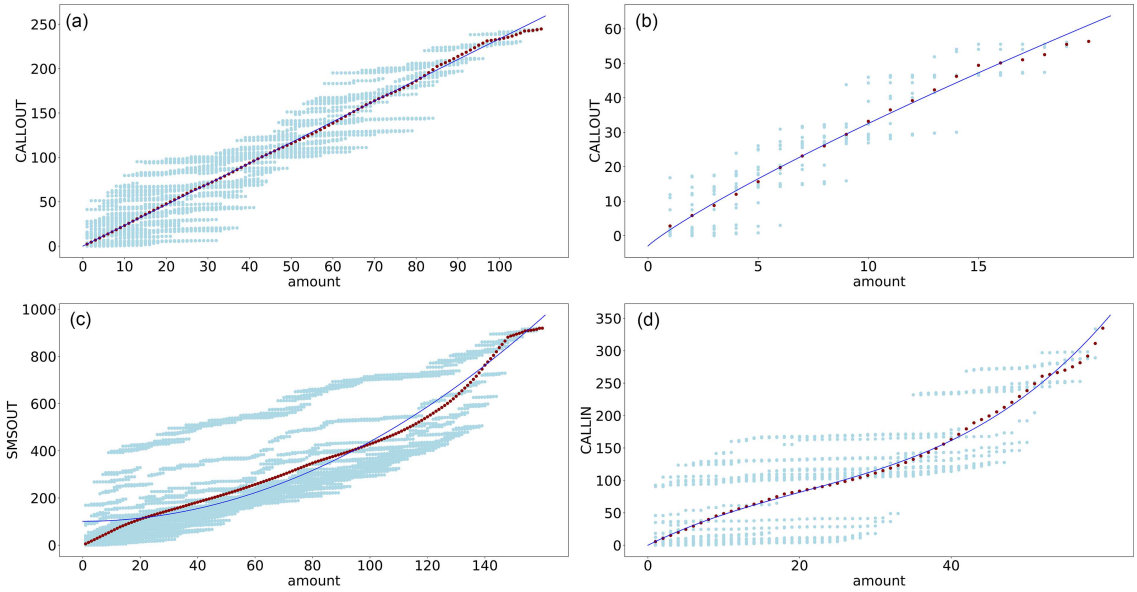

Figure 2 (Color online) Empirical curve fitting results of Metcalfe's law and its variants, which can be considered as $y = an + b$, $y = an \ln n + bn + c$, $y = an^2 + bn + c$, $y = an^3 + bn^2 + cn + d$, corresponding to Sarnoff's, Odlyzko's, Metcalfe's, and cube functions, respectively. The fitted equations in the figure are (a) $y = 2.34\,n$, (b) $y = -0.5\,n \ln n + 4.71\,n - 2.99$, (c) $y = 0.094\,n^2 + 74.65$, and (d) $y = 0.0021\,n^3 - 0.129\,n^2 + 5.82\,n$. In each subfigure, the light blue dots represent the empirical traffic values from real-world data, and the red dots indicate their averages at each network size. The blue curve shows the fitted function, illustrating how well each theoretical model captures the scaling behavior of network traffic load.

enable information exchange. For $\mathfrak{s}$ within $[0, 1)$, the network is characterized as having a more open structure with a larger node base, which affects the rate of data arrival. These findings indicate that Metcalfe's law holds true for this state.

Zhang et al. [10] conducted an empirical study using data from two prominent social network entities, Facebook and Tencent, to validate the principles of Metcalfe's law. Through this research, we emphasize the wide-ranging applicability of Metcalfe's law, as it effectively captures network growth across diverse parameter spaces. The findings reveal that the fundamental mechanisms underlying Metcalfe's law remain applicable to diverse social network environments, offering a robust theoretical basis for analyzing and forecasting network behavior and value.

Metcalfe's law and its variations were verified using a dataset of real-world scenarios [39], which revealed distinct functional relationships in traffic under varying node quantities and diverse scenarios. Metcalfe's law and its variants were successfully fitted by performing random selections and averaging the different node quantities, as shown in Figure 2. We empirically validate these laws by combining our results with previous findings [6, 10, 23].

In this section, we offer an in-depth explanation of the variants of Metcalfe's law. Based on the theoretical findings, we establish connections between these different families of laws, identifying exemplary theoretical cases and real-world scenarios in which they are applicable.

Here, we provide a concise introduction to the recurrence of the Metcalfe's law family. Considering the influence of increasing the number of network nodes on the data arrival rate λ, we assume that λ is a nondecreasing function of n. In the analysis, we explore the different scaling behaviors for λ, specifically $\Theta(1)$, $\Theta(n^{1/2})$, and $\Theta(n)$. Based on these theoretical findings, we match different laws with their exemplary possible cases, respectively. We use these cases to explain the real-world implications of these laws and provide insights into Metcalfe's law and its variants. From Table 1, we can derive other laws corresponding to the different cases. We consider the conditions of several other laws corresponding to different parameter settings while maintaining $\lambda = \Theta(1)$ and $\mathfrak{g} = 0$, as shown in Figure 3 to demonstrate the importance of Metcalfe's law. Detailed data selection and parameter fitting for the functions are provided in Table 3.

5.1 Sarnoff's law: n

5.1.1 *Theoretical cases of Sarnoff's law*

These scenarios for Sarnoff's law are characterized by strong regional correlations and low-degree distributions. In networks characterized by limited openness, interactions between nodes are more constrained, particularly when node activity levels are relatively low. Consequently, the amount of data transmitted between the nodes within a

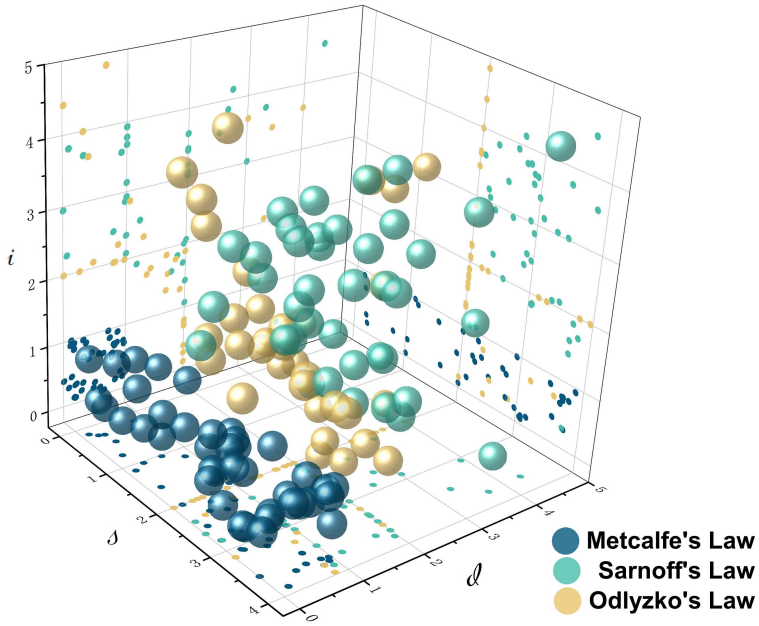

Figure 3 (Color online) Scope of different laws corresponds to the conditions while $\lambda = \Theta(1)$. Notably, the region associated with Metcalfe's law is the most concentrated. We remark that under the condition $\lambda = \Theta(1)$, the cube law has no corresponding conditions. Each axis represents the range of the exponent in the distribution conditions.

Table 3 Empirical results of Metcalfe's law and its variants.

	Given day	Number of nodes n	Interaction types	Value function
Sarnoff's function	3	110	Call-out	$\mathrm{L}_{\mathrm{N}}^{*}(n) = 2.34n$
Odlyzko's function	4	20	Call-out	$\mathrm{L}_{\mathrm{N}}^{*}(n) = -0.5n\ln n + 4.71n - 2.99$
Metcalfe's function	25	80	Call-out	$\mathrm{L}_{\mathrm{N}}^{*}(n) = 0.094n^2 + 74.65$
Cube function	12	60	Call-in	$\mathrm{L}_{\mathrm{N}}^{*}(n) = 0.0021n^3 - 0.129n^2 + 5.82n$

given period is significantly reduced. The use of a constant level of λ in such scenarios is reasonable.

In such networks, the flow of information between nodes is impeded by constrained interactions, which may stem from factors such as device access permissions. Consequently, the overall level of data transmission remains minimal, with only limited exchange occurring among nodes.

5.1.2 *Practical analysis on Sarnoff's law*

The conditions for Sarnoff's law primarily apply to networks with strong localization and a large but limited number of active users, leading to minimal node overlap. Originally formulated for broadcast media platforms, such as TVs or e-mails [5], these networks have limited user interaction, focusing on one-way information transmission from broadcasting nodes to viewers. Hence, the network traffic and value depend linearly on the number of nodes.

In broadcast media networks, the value of a network is closely linked to the number of nodes, instead of the level of user interaction or engagement. The main focus is the dissemination of content from a central source to a large audience, with minimal direct interaction between viewers. The value of these networks is primarily measured by the reach and size of their audiences.

5.2 Odlyzko's law: $n \log n$

5.2.1 *Theoretical cases of Odlyzko's law*

The conditions characterizing Odlyzko's law include dense local connectivity within a limited region, a large number of potential nodes, and relatively few destinations for each node.

This set of conditions is associated with networks that exhibit strong localization, where the majority of nodes have limited connections, and fewer active nodes are present. In such networks, the value of the network primarily stems from the potential user base instead of from active user engagement. Odlyzko's law challenges Metcalfe's law

by emphasizing that the value growth of communication networks is not solely dependent on the number of active connections but also considers the potential reach of the network.

The applicability of Odlyzko's law is contingent on the specific conditions outlined above. These conditions highlight the characteristics of networks in which value growth is driven primarily by the potential user base instead of the level of active engagement.

5.2.2 *Practical analysis on Odlyzko's law*

A typical example is a carrier network [6]. In carrier networks, it is a common practice for large ISPs to reduce peering arrangements with smaller operators. These networks demonstrate pronounced localization, substantial user-base potential, and relatively low user activity levels. In this context, the primary emphasis is on interoperator connectivity. Extensive user-to-user interconnections are minimal. Consequently, the overall number of actively participating nodes in a network remains limited.

Unlike the conditions outlined in Sarnoff's law, networks guided by Odlyzko's law exhibit a slightly elevated level of interactivity. In general, user-to-user interconnections within a network are limited or almost nonexistent. Consequently, the network architecture mainly supports inter-operator connectivity instead of direct user interactions. In this context, the number of actively engaged nodes was constrained.

When considering these attributes, it is reasonable to introduce a factor of $\log n$ to capture the slightly increased interactivity relative to Sarnoff's law. This factor acknowledges the logarithmic growth in network effects stemming from constrained interconnections among users within these networks [6].

5.3 Cube law: n^3

5.3.1 *Theoretical cases of cube law*

As the number of users increases, the amount of incoming information within a unit of time may approach the total number of users, as demonstrated by data from [23].

This trend emphasizes the importance of considering the growing user count when analyzing information flow in networks. With an expanding user base, the network becomes more vibrant, fostering increased interaction and information sharing among users. The continuous growth in user numbers amplifies the rate of information arrival, underscoring the notion that user interactions become increasingly intertwined as the user base expands.

5.3.2 *Practical analysis on cube law*

Several factors contributed to this phenomenon. First, a larger user base in the network leads to more active participants. As more users engage in generating and sharing information, the overall rate of information arrival increases. This data influx contributes to a dynamic and vibrant network ecosystem.

Moreover, with an increase in the number of nodes in the network, we observed a shift in the relationship between network value and network traffic. The traditional linear correlation was surpassed by the network scale. Real-world scenarios, particularly in online social networks, exemplify this trend [23]. Each new user joining the network brings a wealth of additional content, connections, and interactions, all of which contribute to an enhanced user experience. This positive user experience attracts additional users to the network, forming a positive feedback loop that amplifies its value.

Furthermore, economies of scale play a significant roles in this phenomenon. As the number of users increases, the network infrastructure and resources become more efficient and cost-effective. This, in turn, enables the network to handle higher traffic loads [40] and accommodate a growing user base without compromising the performance.

The cube law suggests a highly interconnected network in which users actively exchange information and contribute to the overall network value. This further reinforces the notion that a larger user base results in greater economies of scale, driving the growth and efficiency of networks.

6 Discussion

To further illustrate the relevance of the proposed architecture to real-world networks and its alignment with Metcalfe's law family, this section highlights three essential aspects: the generality of the network model, the suitability of the uniform distribution, and the conceptualization of traffic load as a proxy for network value.

• In this model, each individual node within the network possesses the capability to not only act as a data receiver but also as a data source. This assumption is supported by empirical evidence from real-life scenarios. Across the spectrum of communication technologies, ranging from the deployment of 4G in mobile Internet to the

revolutionary implementation of 5G in the Internet of Things, the dual functionality of network nodes has been consistently manifested. The introduction of this generic model provides numerous possibilities for information dissemination, collaborative data exchange, and peer-to-peer communication.

• In this study, we adopt a uniform distribution for the network geography, primarily for analytical feasibility. As discussed in Appendix B, such a distribution can indeed be observed in real-world scenarios, particularly in the context of social user networks. Although extending the analysis to more general geographic distributions would improve the realism of the model, it would also introduce considerable complexity, which may hinder further analytical progress. Therefore, we leave this direction for future work in which simulation-based approaches will be employed to investigate the effects of more heterogeneous spatial distributions.

• In this study, we quantify the network value using the network traffic load, because both are generated by the demands of the network nodes. The prevailing consensus suggests that *traffic is valued*. We adopt the assumption of a linear relationship between the network value and traffic load, which is a crucial basis for drawing conclusions. However, in the cube law, the scenario is more inclined toward large-scale networks. In such cases, the value generated by network traffic may be significantly greater, potentially breaking the linear relationship between network traffic and value. We recognize the necessity of embarking on future research endeavors aimed at establishing a rigorous and well-defined measurement standard for network value.

7 Conclusion

This study focused on providing the mechanisms and models behind Metcalfe's law and its variants from the perspective of network traffic load. To address the limitations of these laws, potential theoretical conditions under which Metcalfe's law and its variants hold are established, and these laws are correlated with real-world scenarios. The analysis revealed that these laws are applicable to distinct scenarios and have unique significance. We present theoretical results across the complete parameter space for a general network model, offering valuable insights for exploring scenarios associated with the discovery of new scaling laws in the future.

Acknowledgements This work was supported in part by National Natural Science Foundation of China (Grant Nos. 62372328, 72342026), Fundamental Research Funds for the Central Universities (Grant Nos. 22120240357, 2024-1-ZD-04), Key Laboratory of Computing Power Network and Information Security, Ministry of Education (Grant No. 2024ZD001), and Leadership Project under the Eastern Talent Program.

References

1 Gilder G. Metcalfe's law and legacy. Forbes ASAP, 1993, 152: 158–159
2 Ross P E. Commandments: the rules engineers live by weren't always set in stone. IEEE Spectrum, 2003, 40: 30–35
3 Kaprowski G. FCC chair wants universal net access-and he's serious. Wired News, 1996. https://www.wired.com/1996/11/fcc-chair-wants-universal-net-access-and-hes-serious/
4 Reed D P. That Sneaky exponential-Beyond Metcalfes law to the power of community building. Context Magazine, 1999. https://www.downes.ca/post/1562
5 Swann G M P. The functional form of network effects. Inf Economics Policy, 2002, 14: 417–429
6 Briscoe B, Odlyzko A, Tilly B. Metcalfe's law is wrong-communications networks increase in value as they add members-but by how much? IEEE Spectrum, 2006, 43: 34–39
7 Madureira A, den Hartog F, Bouwman H, et al. Empirical validation of Metcalfe's law: how Internet usage patterns have changed over time. Inf Economics Policy, 2013, 25: 246–256
8 Metcalfe B. Metcalfe's Law after 40 years of Ethernet. Computer, 2013, 46: 26–31
9 Van Hove L. Metcalfe's law: not so wrong after all. Netnomics, 2014, 15: 1–8
10 Zhang X Z, Liu J J, Xu Z W. Tencent and Facebook data validate Metcalfe's law. J Comput Sci Tech, 2015, 30: 246–251
11 Wang X, Fu L, Kang H, et al. Revisiting network value: sublinear knowledge law. ArXiv:2304.14084
12 Hendler J, Golbeck J. Metcalfe's law, web 2.0, and the semantic web. J Web Semant, 2008, 6: 14–20
13 Alabi K. Digital blockchain networks appear to be following Metcalfe's law. Electron Commerce Res Appl, 2017, 24: 23–29
14 Peterson T. Metcalfe's Law as a model for bitcoin's value. Alternat Invest Anal Rev Q, 2018, 2: 9–18
15 Wheatley S, Sornette D, Huber T, et al. Are Bitcoin bubbles predictable? Combining a generalized Metcalfe's law and the log-periodic power law singularity model. R Soc Open Sci, 2019, 6: 180538
16 Jung G, Lee B. How did Facebook outspace Myspace with open innovation? An analysis of network competition with changes of network topology. In: Proceedings of Pacific Asia Conference on Information Systems, 2011
17 Scala A, Delmastro M. The explosive value of the networks. Sci Rep, 2023, 13: 1037
18 Ma R, Lin Y, Lin B. Does digitalization support green transition in Chinese cities? Perspective from Metcalfe's law. J Clean Prod, 2023, 425: 138769
19 Tang L, Zhang Y. A study on value assessment of e-commerce enterprises based on the model of real options. Acad J Business Manag, 2023, 5: 118–129
20 Assif M, Kennedy W, Saniee I. Fair allocation in crowd-sourced systems. Games, 2023, 14: 57
21 Moro-Visconti R. Smart healthcare digital transformation during the Covid-19 pandemic. In: Proceedings of Digital Transformation in Healthcare in Post-COVID-19 Times, 2023. 111–132
22 Nowak S. The social lives of network effects: speculation and risk in Jakarta's platform economy. Environ Plan A, 2023, 55: 471–489
23 Zhang X Z, Xu Z W. Facebook and Tencent data fit a cube law better than Metcalfe's law. J Comput Sci Tech, 2023, 38: 219–227
24 Rajgopal S, Venkatachalam M, Kotha S. Why is web traffic value-relevant for internet firms? Retrieved Oct, 2001, 1: 1–31
25 Grégoire J C. Measuring and billing user internet traffic. In: Proceedings of the 6th EURO-NGI Conference on Next Generation Internet, 2010. 1–7
26 Singh R, Agarwal S, Calder M, et al. Cost-effective cloud edge traffic engineering with cascara. In: Proceedings of the USENIX Symposium on Networked Systems Design and Implementation, 2021. 201–216
27 Yang C, You J, Yuan X, et al. Network bandwidth allocation problem for cloud computing. ArXiv:2203.06725

28 Jalaparti V, Bliznets I, Kandula S, et al. Dynamic pricing and traffic engineering for timely inter-datacenter transfers. In: Proceedings of the 2016 ACM SIGCOMM Conference, 2016. 73–86
29 Roy D, Dutta S, Datta A, et al. A cost effective architecture and throughput efficient dynamic bandwidth allocation protocol for fog computing over EPON. IEEE Trans Green Commun Netw, 2020, 4: 998–1009
30 Wang C, Zhang S, Chen Y, et al. Joint configuration adaptation and bandwidth allocation for edge-based real-time video analytics. In: Proceedings of the IEEE INFOCOM 2020-IEEE Conference on Computer Communications, 2020. 257–266
31 Zhao P, You J, Yuan X. Circling reduction algorithm for cloud edge traffic allocation under the 95th percentile billing. IEEE ACM Trans Networking, 2024, 32: 4254–4269
32 Franceschetti M, Dousse O, Tse D N C, et al. Closing the gap in the capacity of wireless networks via percolation theory. IEEE Trans Inform Theory, 2007, 53: 1009–1018
33 Grimmett G, Grimmett G. What is Percolation? New York: Springer, 1999
34 Wang C, Tang S, Yang L, et al. Modeling data dissemination in online social networks: a geographical perspective on bounding network traffic load. In: Proceedings of the 15th ACM International Symposium on Mobile Ad Hoc Networking and Computing, 2014. 53–62
35 Kleinberg J M. Navigation in a small world. Nature, 2000, 406: 845
36 Liben-Nowell D, Novak J, Kumar R, et al. Geographic routing in social networks. Proc Natl Acad Sci USA, 2005, 102: 11623–11628
37 Manning C, Schütze H. Foundations of Statistical Natural Language Processing. Cambridge: MIT Press, 1999
38 Sala A, Zheng H, Zhao B Y, et al. Brief announcement: revisiting the power-law degree distribution for social graph analysis. In: Proceedings of the 29th ACM SIGACT-SIGOPS Symposium on Principles of Distributed Computing, 2010. 400–401
39 Barlacchi G, De Nadai M, Larcher R, et al. A multi-source dataset of urban life in the city of Milan and the Province of Trentino. Sci Data, 2015, 2: 1–5
40 Cui Q M, You X H, Wei N, et al. Overview of AI and communication for 6G network: fundamentals, challenges, and future research opportunities. Sci China Inf Sci, 2025, 68: 171301
41 Steele J. Growth rates of Euclidean minimal spanning trees with power weighted edges. Ann Probab, 1988, 16: 1767–1787
42 Williams D. Probability with Martingales. Cambridge: Cambridge University Press, 1991
43 Wang C, Zhang Z, Zhou J, et al. Modeling interest-driven data dissemination in online social networks. In: Proceedings of the 2016 12th International Conference on Mobile Ad-Hoc and Sensor Networks, 2016. 290–295
44 Gilbert E N, Pollak H O. Steiner minimal trees. SIAM J Appl Math, 1968, 16: 1–29
45 Penrose M. A strong law for the longest edge of the minimal spanning tree. Ann Probab, 1999, 27: 246–260

Appendix A Theoretical foundations and implications

Appendix A.1 Theoretical analysis

In this section, we present a detailed analysis of the traffic load quantification in a network. We present a comprehensive model that enables us to quantify traffic loads and derive meaningful insights. We provide proofs to support our conclusions to validate these findings.

Appendix A.1.1 *Basic lemmas*

Lemma 1 (Minimal spanning tree [41])**.** Let X_i, $1 \leqslant i < \infty$, denote independent random variables with values in $\mathbb{R}^d$, $d \geqslant 2$, and let M_n denote the cost of a minimal spanning tree of a complete graph with vertex set $\{X_i\}_{i=1}^n$, where the cost of edge (X_i, X_j) is given by $\Psi((|X_i - X_j|))$. Here, $|X_i - X_j|$ denotes the Euclidean distance between X_i and X_j and Ψ denotes a monotonic function. For bounded random variables and $0 < \sigma < d$, it holds that, as $n \to \infty$, with probability 1, we have

$$M_n \sim c_1(\sigma, d) \cdot n^{\frac{d-\sigma}{d}} \cdot \int_{\mathbb{R}^d} f(X)^{\frac{d-\sigma}{d}} dX,$$

provided that $\Psi(x) \sim x^\sigma$, where $f(X)$ denotes the density of the absolutely continuous part of the distribution of $\{X_i\}$.

Lemma 2 (Kolmogorov's strong LLNs [42])**.** Let $\{X_n\}$ be an i.i.d. sequence of random variables having finite mean. For $\forall n$, $\mathbb{E}[X_n] < \infty$. Then, the strong law of large numbers (LLNs) is applied to the sample mean:

$$\bar{X}_n \xrightarrow{\text{a.s.}} \mathbb{E}[X_n],$$

where $\xrightarrow{\text{a.s.}}$ denotes *almost sure convergence*.

Lemma 3. For $k = 1, 2, \ldots, n$, it holds that

$$\mathrm{L}_{\mathrm{N}}^* = \lambda \cdot \Omega \left(\sum_{k=1}^{n} |\operatorname{EMST}(\{u_k\} \cup \mathbb{D}_k)| \right),$$

where $\operatorname{EMST}(\cdot)$ denotes the EMST over a set.

See Lemma 1 in [34] for the proof of this lemma.

Lemma 4. Consider the Zipf's distribution whose distribution function is $\Pr(q_k = q) = \left(\sum_{j=1}^{n-1} j^{-\alpha}\right)^{-1} \cdot q^{-\alpha}$, where α is a parameter describing the distribution. We obtain that

$$\Pr(q_k = q) = \begin{cases} \Theta\left(q^{-\alpha}\right), & \alpha > 1, \\ \Theta\left(\dfrac{1}{\log n} \cdot q^{-1}\right), & \alpha = 1, \\ \Theta\left(n^{\alpha-1} \cdot q^{-\alpha}\right), & 0 < \alpha < 1. \end{cases} \tag{A1}$$

Appendix A.1.2 *Euclidean minimum spanning tree*

Let a network session be an ordered pair $\mathrm{T}_k = \langle v_k, \mathcal{A}_k \rangle$, where v_k denotes the source and each element v_{k_i} in $\mathcal{A}_k = \{v_{k_i}\}_{i=1}^{r_k}$ is the nearest node to the corresponding p_{k_i} in $\mathfrak{d}_k^{\mathrm{I}} = \{p_{k_i}\}_{i=1}^{r_k}$. The random variable r_k denotes the number of potential destinations for session T_k. The destination for node v_k is dynamically selected based on the data transported within the network during the session. We refer to point p_{k_i} as the *anchor point* of v_{k_i} and define a set $\mathcal{P}_k := \{v_k\} \cup \mathcal{A}_k$. Then, we obtain the following lemma.

Lemma 5 (EMST with $\mathfrak{s}$ and r_k [34])**.** For a network broadcast session T_k, when $r_k = \omega(1)$, with probability 1, it holds that

$$|\operatorname{EMST}(\mathcal{A}_k)| = \Theta(L_{\mathcal{P}}(\mathfrak{s}, r_k)),$$

and then

$$|\operatorname{EMST}(\mathcal{P}_k)| = \Omega(L_{\mathcal{P}}(\mathfrak{s}, r_k)),$$

where $\operatorname{EMST}(\cdot)$ denotes the EMST over set,

$$L_{\mathcal{P}}(\mathfrak{s}, r_k) = \begin{cases} \Theta\left(\sqrt{r_k}\right), & \mathfrak{s} > 2, \\ \Theta\left(\sqrt{r_k} \cdot \log n\right), & \mathfrak{s} = 2, \\ \Theta\left(\sqrt{r_k} \cdot n^{1-\frac{\mathfrak{s}}{2}}\right), & 1 < \mathfrak{s} < 2, \\ \Theta\left(\sqrt{r_k} \cdot \sqrt{\frac{n}{\log n}}\right), & \mathfrak{s} = 1, \\ \Theta\left(\sqrt{r_k} \cdot \sqrt{n}\right), & 0 \leqslant \mathfrak{s} < 1. \end{cases} \tag{A2}$$

Proof. With probability 1, it holds that

$$|\operatorname{EMST}(\mathcal{A}_k)| = \Theta(L_{\mathcal{P}}(\mathfrak{s}, r_k)) \text{ for } r_k = \omega(1),$$

where $L_{\mathcal{P}}(\mathfrak{s}, r_k)$ is defined by (A2). Given that

$$|\operatorname{EMST}(\mathcal{P}_k)| \geqslant |\operatorname{EMST}(\mathcal{A}_k)|,$$

we obtain

$$|\operatorname{EMST}(\mathcal{P}_k)| = \Omega(L_{\mathcal{P}}(\mathfrak{s}, r_k)).$$

Next, we focus on the derivation of $L_{\mathcal{P}}(\mathfrak{s}, r_k)$. Given X_0 is a point from $\mathcal{O}$ selected arbitrarily, and X_0 is the reference point. The distribution of the points in $\mathcal{A}_k$ follows the density function:

$$f_{X_0}(X) = \frac{\left(\int_{\mathcal{D}(X_0, |X - X_0|)} \mathbf{d}(Y) dY + 1\right)^{-s}}{\int_{\mathcal{O}} \left(\int_{\mathcal{D}(X_0, |X - X_0|)} \mathbf{d}(Y) dY + 1\right)^{-s} dZ},$$

where $\mathbf{d}(Y) = n \sum_{c_j \in \mathcal{C}} \frac{g(|Y - c_j|)}{\int_{\mathcal{O}} g(|Z - c_j|) dZ}$ and $\mathcal{C}$ are the position sets of the points from [34].

Although we assume that $\mathfrak{g} = 0$, we obtain $g(\cdot) = 1$ and $\mathbf{d}(Y) = 1$. By combining the conclusions of Lemma 4, the density function can be calculated as follows:

$$f_{X_0}(X) = \begin{cases} \Theta\left((|X - X_0|^2 + 1)^{-\mathfrak{s}}\right), & \mathfrak{s} > 1, \\ \Theta\left(\frac{1}{\log n} \cdot (|X - X_0|^2 + 1)^{-1}\right), & \mathfrak{s} = 1, \\ \Theta\left(n^{\mathfrak{s}-1} \cdot (|X - X_0|^2 + 1)^{-\mathfrak{s}}\right), & 0 < \mathfrak{s} < 1. \end{cases}$$

From the value of $\mathfrak{s}$, we can obtain the following results.

(1) When $\mathfrak{s} > 1$,

$$\int_{\mathcal{O}} \sqrt{f_{X_0}(X)} dX = \Theta\left(\int_{\mathcal{O}} \frac{dX}{(|X - X_0|^2 + 1)^{\frac{\mathfrak{s}}{2}}}\right) = \begin{cases} \Theta(1), & \mathfrak{s} > 2, \\ \Theta(\log n), & \mathfrak{s} = 2, \\ \Theta\left(n^{1-\frac{\mathfrak{s}}{2}}\right), & 1 < \mathfrak{s} < 2. \end{cases}$$

(2) When $\mathfrak{s} = 1$,

$$\int_{\mathcal{O}} \sqrt{f_{X_0}(X)} dX = \Theta\left(\frac{1}{\sqrt{\log n}} \cdot \int_{\mathcal{O}} \frac{dX}{(|X - X_0|^2 + 1)^{\frac{1}{2}}}\right) = \Theta\left(\sqrt{\frac{n}{\log n}}\right).$$

(3) When $0 \leqslant \mathfrak{s} < 1$,

$$\int_{\mathcal{O}} \sqrt{f_{X_0}(X)} dX = \Theta\left(n^{\frac{\mathfrak{s}-1}{2}} \cdot \int_{\mathcal{O}} \frac{dX}{(|X - X_0|^2 + 1)^{\frac{\mathfrak{s}}{2}}}\right) = \Theta\left(\sqrt{n}\right).$$

By combining all the above cases, we complete the proof.

Appendix A.1.3 *Proof of Theorem 1*

Here, we present the logical framework for this proof. For conciseness, we refer to several common conclusions from [34,43]. The scenario they studied, which is online social networks, is indeed a special case for this study. Some commonalities still exist in the technical logic.

In the context of the underlying network, the problem of achieving an optimal transmission distance involves connecting the nodes in a given plane, which constitutes the set $\{u_k\} \cup \mathbb{D}_k$, where $\mathbb{D}_k$ represents all destinations of u_k. The total length of the Euclidean spanning tree for a session can be used to gauge the magnitude of the optimal transport distance. This problem can be simplified by generating a Euclidean Steiner tree for the set $u_k \cup \mathbb{D}_k$ [44]. Then, we can deduce that

$$\mathrm{L}_{\mathrm{N}}^{*} = \lambda \cdot \Omega \left(\sum_{k=1}^{n} |\operatorname{EMST}(\{u_k\} \cup \mathbb{D}_k)| \right),$$

where $\operatorname{EMST}(\cdot)$ denotes the EMST [45].

Further, let $\mathcal{A}_k = \{p_{k_1}, p_{k_2}, \ldots, p_{k_{q_k}}\}$ and $\mathcal{F}_k = \{v_{k_1}, v_{k_2}, \ldots, v_{k_{q_k}}\}$ denote the set of q_k nodes and the closest nodes to p_{k_i}, for $1 \leqslant i \leqslant q_k$, respectively. In addition, we denote the set $\mathcal{P}_k = \{v_k\} \cup \mathcal{A}_k$, where v_k is the source from a given session T_k and the anchor point of v_{k_i} is p_{k_i}. Subsequently, for a data transportation session T_k, we obtain

$$|\operatorname{EMST}(\mathcal{A}_k)| = \Theta(L_{\mathcal{P}}(\mathfrak{s}, r_k)), |\operatorname{EMST}(\mathcal{P}_k)| = \Omega(L_{\mathcal{P}}(\mathfrak{s}, r_k)),$$

where $L_{\mathcal{P}}(\mathfrak{s}, r_k) = \sqrt{r_k} \cdot \int_{\mathcal{O}} \sqrt{f_{X_0}(X)} dX$.

In Lemma 5, the result of $L_{\mathcal{P}}(\mathfrak{s}, r_k)$ is given by (A2),

$$L_{\mathcal{P}}(\mathfrak{s}, r_k) = \begin{cases} \Theta\left(\sqrt{r_k}\right), & \mathfrak{s} > 2, \\ \Theta\left(\sqrt{r_k} \cdot \log n\right), & \mathfrak{s} = 2, \\ \Theta\left(\sqrt{r_k} \cdot n^{1-\frac{\mathfrak{s}}{2}}\right), & 1 < \mathfrak{s} < 2, \\ \Theta\left(\sqrt{r_k} \cdot \sqrt{\frac{n}{\log n}}\right), & \mathfrak{s} = 1, \\ \Theta\left(\sqrt{r_k} \cdot \sqrt{n}\right), & 0 \leqslant \mathfrak{s} < 1. \end{cases} \tag{A3}$$

First, we consider the *node influence distribution* and define two sets for all data transportation sessions, where $\mathcal{K}^1$ represents the nodes with a constant level of influence $\Theta(1)$, and $\mathcal{K}^{\infty}$ denotes the nodes with a nonconstant level of influence. Together, these fully characterize $\sum_{k=1}^{n} |\operatorname{EMST}(\mathcal{P}_k)|$. In this proof, Ψ^1 is defined to represent the sum of the lengths of all the EMSTs under the condition $k \in \mathcal{K}^1$, where $\Psi^1 = \sum_{k \in \mathcal{K}^1} |\operatorname{EMST}(\mathcal{P}_k)|$, and Ψ^{∞} is defined to represent the one under the condition $k \in \mathcal{K}^{\infty}$, where $\Psi^{\infty} = \sum_{k \in \mathcal{K}^{\infty}} |\operatorname{EMST}(\mathcal{P}_k)|$.

First, we address Ψ^1. For $q_k = \Theta(1)$, it holds that $|\operatorname{EMST}(\mathcal{P}_k)| = \Theta(|X - v_k|)$. We define a sequence of random variables $\varepsilon_k := |X - v_k|/\sqrt{n}$, and $\mathbb{E}[\varepsilon_k] = \mathbb{E}[|X - v_k|]/\sqrt{n}$. The value of $\mathbb{E}[|X - v_k|]$ is given in Lemma 5 of [34] and $\Psi^1 = \Theta(\sqrt{n} \sum_{k \in \mathcal{K}^1} \varepsilon_k)$. Using Kolmogorov's strong LLNs [42] with probability 1,

$$\Psi^1 = \Theta\left(|\mathcal{K}^1| \cdot E[|X - v_k|]\right).$$

Next, *data destination distribution* is utilized to consider Ψ^{∞}. All $|\operatorname{EMST}(\mathcal{P}_k)|$ are independent, where $k \in \mathcal{K}^{\infty}$, owing to the introduction of anchor points. Similar to the node influence distribution, we apply the same approach to distinguish the number of nodes selected by this distribution. Specifically, we denote Ψ_1^{∞} and Ψ_{∞}^{∞} as the sum of the lengths of all EMSTs under $r_k = \Theta(1)$ and $r_k = \omega(1)$, respectively.

For $r_k = \Theta(1)$, the value of Ψ_1^{∞} is relatively infinitesimal compared with Ψ^1.

Then, we consider $\mathcal{K}_{\infty}^{\infty}$. We define $T_q = n \cdot \Pr(q_k = q) = n \cdot \left(\sum_{j=1}^{n-1} j^{-\mathfrak{i}}\right)^{-1} \cdot q^{-\mathfrak{i}}$, as the number of nodes with q destinations.

Through the LLNs [42], with probability 1, it holds that

$$\Psi_{\infty}^{\infty} \geqslant \sum_{q=2}^{n-1} \sum_{r=1}^{q} T_q \cdot \Pr(r_k = r | q_k = q) \cdot L_{\mathcal{P}}(\mathfrak{s}, r).$$

We calculate $\sum_{q=2}^{n-1} \sum_{r=1}^{q} \Pr(q_k = q) \cdot \Pr(r_k = r | q_k = q)$, denoted by $G(\mathfrak{i}, \mathfrak{d})$, as summarized in Table A1.

Combined with the above conclusions, the lower bounds were obtained for $\sum_{k=1}^{n} |\operatorname{EMST}(\mathcal{P}_k)|$.

Then, we calculate $\sum_{k=1}^{n} |\operatorname{EMST}(\mathbb{D}_k)|$, as

$$\sum_{k=1}^{n} r_k = \Theta\left(\sum_{q=1}^{n-1} \sum_{r=1}^{q} T_q \cdot \Pr(r_k = r | q_k = q) \cdot r \right),$$

where $T_q = n \cdot \Pr(q_k = q)$. We obtain the results for $\sum_{k=1}^{n} r_k$ as $W(\mathfrak{i}, \mathfrak{d})$, as summarized in Table A2.

In addition, for all $u_k \in \mathcal{U}$,

$$E[|v_{k_i} - p_{k_i}|] = \Theta\left(\int_0^{\sqrt{n}} x \cdot \mathrm{e}^{-\pi x^2} dx \right).$$

That is,

$$E[|v_{k_i} - p_{k_i}|] = \Theta(1),$$
$$\sum_{k=1}^{n} \sum_{i=1}^{r_k} |v_{k_i} - p_{k_i}| = \Theta\left(\sum_{k=1}^{n} r_k \right) = \Theta(W(\mathfrak{i}, \mathfrak{d})).$$

By combining the results of $\sum_{k=1}^{n} |\operatorname{EMST}(\mathcal{P}_k)|$ and the data arrival rate λ, we complete the proof.

Table A1 The value of $G(\mathfrak{i},\mathfrak{d})$.

$\mathfrak{d}$	$G(\mathfrak{i},\mathfrak{d})$
$\mathfrak{d}>\frac{3}{2}$	$\Theta(1)$, $\mathfrak{i}\geqslant 0$
$\mathfrak{d}=\frac{3}{2}$	$\begin{cases}\Theta(1), & \mathfrak{i}>1;\\ \Theta(\log n), & 0\leqslant\mathfrak{i}\leqslant 1\end{cases}$
$1<\mathfrak{d}<\frac{3}{2}$	$\begin{cases}\Theta(1), & \mathfrak{i}>\frac{5}{2}-\mathfrak{d};\\ \Theta(\log n), & \mathfrak{i}=\frac{5}{2}-\mathfrak{d};\\ \Theta(n^{\frac{5}{2}-\mathfrak{i}-\mathfrak{d}}), & 1<\mathfrak{i}<\frac{5}{2}-\mathfrak{d};\\ \Theta(n^{\frac{3}{2}-\mathfrak{d}}/\log n), & \mathfrak{i}=1;\\ \Theta(n^{\frac{3}{2}-\mathfrak{d}}), & 0\leqslant\mathfrak{i}<1\end{cases}$
$\mathfrak{d}=1$	$\begin{cases}\Theta(1), & \mathfrak{i}\geqslant\frac{3}{2};\\ \Theta(n^{\frac{3}{2}-\mathfrak{i}}/\log n), & 1<\mathfrak{i}<\frac{3}{2};\\ \Theta(n^{\frac{1}{2}}/(\log n)^2), & \mathfrak{i}=1;\\ \Theta(n^{\frac{1}{2}}/\log n), & 0\leqslant\mathfrak{i}<1\end{cases}$
$0\leqslant\mathfrak{d}<1$	$\begin{cases}\Theta(1), & \mathfrak{i}>\frac{3}{2};\\ \Theta(\log n), & \mathfrak{i}=\frac{3}{2};\\ \Theta(n^{\frac{3}{2}-\mathfrak{i}}), & 1<\mathfrak{i}<\frac{3}{2};\\ \Theta(n^{\frac{1}{2}}/\log n), & \mathfrak{i}=1;\\ \Theta(n^{\frac{1}{2}}), & 0\leqslant\mathfrak{i}<1\end{cases}$

Table A2 The number of all destinations, $W(\mathfrak{i},\mathfrak{d})$.

$\mathfrak{d}$	$W(\mathfrak{i},\mathfrak{d})$
$\mathfrak{d}>2$	$\Theta(n)$, $\mathfrak{i}\geqslant 0$
$\mathfrak{d}=2$	$\begin{cases}\Theta(n), & \mathfrak{i}>1;\\ \Theta(n\cdot\log n), & 0\leqslant\mathfrak{i}\leqslant 1\end{cases}$
$1<\mathfrak{d}<2$	$\begin{cases}\Theta(n), & \mathfrak{i}>3-\mathfrak{d};\\ \Theta(n\cdot\log n), & \mathfrak{i}=3-\mathfrak{d};\\ \Theta(n^{4-\mathfrak{i}-\mathfrak{d}}), & 1<\mathfrak{i}<3-\mathfrak{d};\\ \Theta(n^{3-\mathfrak{d}}/\log n), & \mathfrak{i}=1;\\ \Theta(n^{3-\mathfrak{d}}), & 0\leqslant\mathfrak{i}<1\end{cases}$
$\mathfrak{d}=1$	$\begin{cases}\Theta(n), & \mathfrak{i}\geqslant 2;\\ \Theta(n^{3-\mathfrak{i}}/\log n), & 1<\mathfrak{i}<2;\\ \Theta(n^2/(\log n)^2), & \mathfrak{i}=1;\\ \Theta(n^2/\log n), & 0\leqslant\mathfrak{i}<1\end{cases}$
$0\leqslant\mathfrak{d}<1$	$\begin{cases}\Theta(n), & \mathfrak{i}>2;\\ \Theta(n\cdot\log n), & \mathfrak{i}=2;\\ \Theta(n^{3-\mathfrak{i}}), & 1<\mathfrak{i}<2;\\ \Theta(n^2/\log n), & \mathfrak{i}=1;\\ \Theta(n^2), & 0\leqslant\mathfrak{i}<1\end{cases}$

Appendix A.2 How to understand the results

The visual results were conditioned on multiple distribution indices, as shown in Figure A1. The theoretical depiction of traffic load manifests breakpoints regardless of the conditions, signifying potential "phase transitions" in real-world scenarios owing to varying conditions. These breakpoints play a pivotal role in delineating distinct shifts or transformations within network dynamics. This observation parallels the existence of multiple variants of Metcalfe's law, suggesting the presence of diverse breakpoints and transitions, thereby underlining the crucial role of these breakpoints.

Appendix B Empirical evaluations on network geography distribution

In this section, the geographical distribution of the network is evaluated using the Gowalla dataset. The Gowalla dataset is a comprehensive collection of location-based information obtained from the Gowalla social networking platform. It predominantly emphasizes geospatial data associated with check-ins and user activities across diverse physical locations. Each check-in record generally encompasses details, such as the geographical coordinates (latitude and longitude) of the location, timestamp, and occasionally supplementary metadata, such as the name or venue category of the place.

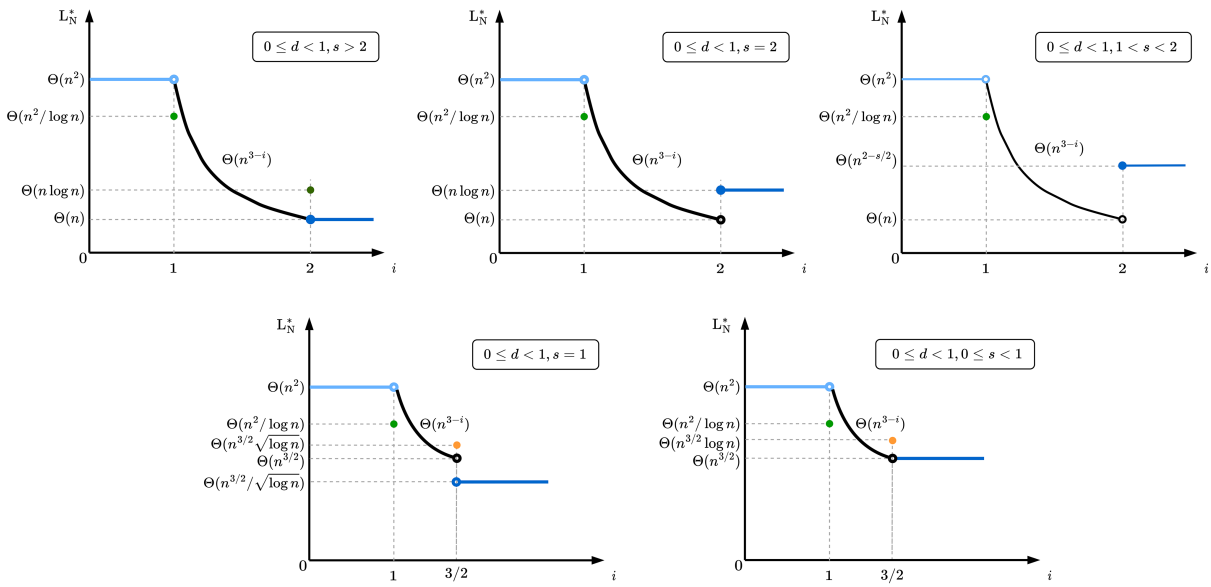

Figure A1 (Color online) Order of lower bounds on the derived traffic load, under $\lambda = \Theta(1)$ and $0 \leqslant \mathfrak{d} < 1$.

We present the overall geographical distribution of Gowalla users in the United States using a Mercator projection coordinate system[1)]. Building on this, we selected two specific locations to examine the distribution of the geographical positions, providing further clarification of the configurations. Subsequent to a detailed analysis of the dataset, a noticeable trend emerged: the geographical distribution within real-world networks tendeds to favor uniformity. This observation supports the credibility of our underlying assumptions.

Appendix C Origin and evolution of this work

Here, we elaborate on the origin and evolution of our study. First, we studied the scaling laws for the traffic loads in online social networks. We proposed a three-layer model comprising a physical network layer, a social relationship layer, and an application session layer, enabling us to determine the scale of the traffic load within this model [34]. This breakthrough addressed the analytical challenges of bridging the physical network layer and the application session layer. Furthermore, we addressed this deficiency [43]. We proposed a three-layer model comprising the physical network layer, a social relationship layer, and application session layer, enabling us to determine the scale of the traffic load within this model. This breakthrough addressed the analytical challenges of bridging the physical network layer and application session layer. Since then, we have worked on projects related to network engineering, gradually focusing on the value of networks, including Metcalfe's law. After further investigation, we found that several variants of Metcalfe's law exist, creating a debate over which scaling laws provide greater representation. A possible reason for this is that these laws are applicable to different scenarios. Therefore, theoretically describing the differences between such scenarios is difficult. After determining the possible relationship between traffic and value, we hope that previous work can be used to explain Metcalfe's law and its variants. However, when we attempted to explain Metcalfe's law and its variants using our previous work, we encountered two difficulties. First, our network model summarizes the commonalities and applies them to more general networks. Second, previous studies lack rigorous theoretical proofs across general system models. To address these challenges, we devised a general network model and introduced different distributions for the different layers. In addition, we presented possible models and mechanisms underlying the emergence of Metcalfe's law and its variants from the perspective of network traffic load. Theoretical analysis revealed that these laws are applicable in distinct scenarios and have unique significance, offering valuable insights for exploring scenarios associated with the discovery of new scaling laws beyond those mentioned above in the future.

1) Details can be seen in https://github.com/YiWang1d2/MetcalfesLaw.